ORIGINAL RESEARCH

MicroRNA-26a Protects the Heart Against Hypertension-Induced Myocardial Fibrosis

Wenqian Zhang, MD*; Qiaozhu Wang, MD*; Yanjing Feng, PhD; Xuegui Chen, MSc; Lijun Yang, MD; Min Xu, MD; Xiaofang Wang, PhD; Weicheng Li, MSc; Xiaolin Niu, MD; Dengfeng Gao (ID), MD, PhD

BACKGROUND: Hypertensive myocardial fibrosis (MF) is characterized by excessive deposition of extracellular matrix and cardiac fibroblast proliferation, which can lead to heart failure, malignant arrhythmia, and sudden death. In recent years, with the deepening of research, microRNAs have been found to have an important role in blood pressure control and maintaining normal ventricular structure and function.

METHODS AND RESULTS: In this study, we first documented the downregulation of microRNA-26a (miR-26a) in the plasma and myocardium of spontaneously hypertensive rats; more importantly, miR-26a–deficient mice showed MF, whereas overexpression of miR-26a significantly prevented elevated blood pressure and inhibited MF in vivo and angiotensin II-induced fibrogenesis in cardiac fibroblasts by directly targeting connective tissue growth factor and Smad4. miR-26a inhibited cardiac fibroblast proliferation by the enhancer of zeste homolog 2/p21 pathway.

CONCLUSIONS: Our study identified a novel role for miR-26a in blood pressure control and hypertensive MF and provides a possible treatment strategy for miR-26a to alleviate and reverse hypertensive MF.

Key Words: hypertension ■ microRNA-26a ■ myocardial fibrosis

Primary hypertension is a major risk factor for the development of cardiovascular disease, one of the leading causes of mortality and morbidity. About 1 billion people in the world have primary hypertension.[1] High blood pressure (BP) damages the compliance and induces pressure overload of the heart, which goes along with fibrotic remodeling and then detrimentally affects left ventricular structure and function.[2,3] Myocardial fibrosis (MF) in hypertension is associated with increased risk of heart failure, cerebrovascular accidents, and arrhythmia.[4–6] Therefore, exploring novel and powerful treatments for hypertension and seeking new therapeutic targets for hypertensive MF at the molecular level has become important.[7]

MicroRNAs (miRNAs), of approximately 18 to 25 nt, belong to the non-protein–coding RNAs. They bind to the 3' or 5' untranslated (UTR) region of specific target gene mRNA to negatively regulate target gene expression after transcription by the principle of complete or incomplete complementary base pairing. miRNAs affect a wide variety of biological functions ranging from development to disease.[8,9] They may participate in the development of hypertensive MF.[10,11]

miRNA-26a (miR-26a) is a highly conserved post-transcriptional regulator in various cellular processes, including proliferation, differentiation, migration, and apoptosis.[12] A large number of studies have shown that miR-26a genes are closely related to cardiovascular diseases.[12,13] Meanwhile, miR-26a could ameliorate the severity of fibrosis in organs other than the heart, including liver, lung, and lens.[14–16] However, the role of miR-26a in hypertensive MF has not been reported.

In the present study, we investigated the expression of miR-26a in hypertensive animal models and

CLINICAL PERSPECTIVE

What Is New?

- MicroRNA-26a (miR-26a) inhibits hypertension-induced myocardial fibrosis in vivo and angiotensin II-induced fibrogenesis in cardiac fibroblasts and prevents blood pressure elevation in spontaneously hypertensive rats.
- MiR-26a reduces collagen, extracellular matrix deposition by directly targeting connective tissue growth factor and inhibits transforming growth factor β/Smad signal pathway by directly targeting Smad4.
- MiR-26a inhibits cardiac fibroblast proliferation by the enhancer of zeste homolog 2/p21 pathway.

What Are the Clinical Implications?

- Our study reveals a novel role for miR-26a in hypertension-induced myocardial fibrosis and blood pressure control.
- We provide a possible treatment strategy for miR-26a in alleviating and reversing hypertension-induced myocardial fibrosis.

Nonstandard Abbreviations and Acronyms

AngII	angiotensin II
CF	cardiac fibroblast
Col	collagen
CTGF	connective tissue growth factor
ECM	extracellular matrix
EZH2	enhancer of zeste homolog 2
MF	myocardial fibrosis
miR-26a	microRNA-26a
miRNA	microRNA
MMP2	matrix metalloproteinase 2
MuT	mutant-type
qPCR	quantitative real-time polymerase chain reaction
rAAV	recombinant adeno-associated virus
SBP	systolic blood pressure
SHR	spontaneously hypertensive rat
TGFβRI	transforming growth factor βRI
WKY	Wistar-Kyoto rat
WT	wild type

observed MF in miR-26a knockout mice. Then we used recombinant adeno-associated virus- (rAAV-) miR-26a to upregulate the expression of miR-26a in spontaneously hypertensive rats (SHRs) and observed the change in BP and related cardiac-specific protein. Meanwhile, we used a miR-26a mimic or inhibitor to intervene in angiotensin II- (AngII-) induced cardiac fibroblasts (CFs) to observe fibrogenesis and proliferation. Illuminating the role of miR-26a in hypertension-induced MF may help in understanding the underlying molecular mechanism and suggest potential therapeutic targets.

METHODS

The data that support the findings of this study are available from the corresponding author upon reasonable request.

Animals and Experimental Protocols

Male miR-26a$^{+/-}$ mice (n=4; age 18–20 weeks; weight 30±3 g) were purchased from the Bioray Laboratory (Shanghai, China). Male miR-26a$^{+/+}$ mouse littermates served as controls (n=4; age 18–20 weeks; weight 30±3 g). Hearts were harvested rapidly from euthanized mice after rapid cervical dislocation. Male SHRs and Wistar-Kyoto rats (WKYs) were purchased from Beijing Wei Tong Lihua Experimental Animal Center (Beijing, China). First, we used SHRs that were 8 weeks old (n=6, weight, 210±10 g) and 16 weeks old (n=6, weight, 300±20 g), and WKYs that were 8 weeks old (n=6, weight, 220±10 g) and 16 weeks old (n=6, weight, 270±20 g) for BP measurement after 3 days of adaptation. Then animals were anesthetized by isoflurane inhalation (1%–2.5%), and plasma and hearts were collected. For the rAAV transfection experiment, we used 7-week-old SHRs (190±10 g) and WKYs (200±10 g). After 1 week of adaptation, SHRs were randomly divided into 3 groups: rAAV-miR-26a–treated group (rAAV-miR-26a, n=8): rAAV-GFP-miR-26a (Han Heng Biotechnology Co, Shanghai, China; 150 µL, 2×10^{11} viral genome); vector controls (rAAV-GFP, n=8): rAAV-GFP (Han Heng Biotechnology Co; 150 µL, 2×10^{11} viral genome); and vehicle controls (SHR-Ctrl, n=8): normal saline (150 µL). WKYs were normal controls (WKY, n=6): normal saline (150 µL). The rAAV vectors or normal saline was administered via tail vein bolus injection at a uniform rate for 5 seconds. The rAAV vectors we used were rAAV of type 9. The rats had 1 injection on day 1; after 3 weeks, the rats were euthanized by cervical dislocation and hearts were excised. Animals were housed in a room with light/dark cycle 12/12 hours, relative humidity of 50% to 60%, ambient temperature 22 to 25°C, 4 to 5 rats or mice per cage, with free access to food and water. All procedures were approved by the Animal Care and Use Committee at Xi'an Jiao Tong University (Xi'an, Shaanxi, People's Republic of China) and conformed to National Institute of Health (NIH, Bethesda, MD) guidelines.

Blood Pressure Measurements

Systolic blood pressure (SBP) was measured by a tail-cuff method with conscious rats by using a noninvasive BP-analysis system (BP-2000 SERIESII; Visitech Systems, Apex, NC). Before measurement, rats were placed in a holding device (37°C) for 5 minutes. SBP was determined at least 3 times; mean values were used as the result. Before the intervention, SBP of the caudal artery was recorded and SBP was measured every 3 to 5 days during the intervention period until the experiment's end.

Morphological Analysis

Cardiac sections were fixed in 4% paraformaldehyde, then embedded in paraffin. Sections of 5-µm thickness were stained with hematoxylin and eosin to evaluate morphology and cellular dimensions. Photomicrographs were obtained by light microscopy (DS-Fi1-Eclipse; Nikon, Tokyo, Japan). Myocardial collagen was stained with Masson's trichrome. Photomicrographs were analyzed in a blinded manner. Photographs of left ventricular sections cut from the posterior inferior septal of each heart were used for morphometric analysis. Changes in myocardial interstitial collagen were observed by using a microscopy imaging system (DS-Fi1-Eclipse; Nikon). MF was quantified by measuring the blue fibrotic area. Collagen volume fraction refers to the ratio of the area of collagen relative to the total area of the image. Ten fields at high magnification (×400) were randomly taken and areas of collagen were calculated.

Immunohistochemical Staining

The proliferative activity of cells was determined by using Ki-67 antibody (1:500 dilution; Servicebio Technology Co, Ltd, Wuhan, China). Each slide was analyzed by confocal microscopy (DS-Fi1-Eclipse; Nikon). The total number of Ki-67+ cells and total nuclei was counted from each image. Cells with brown staining were defined as Ki-67+. The proliferation index was determined by dividing the number of Ki-67+ nuclei by the total number of sampled nuclei. Ten fields at high magnification (×400) were randomly taken from every section.

Cell Culture and Transfection

CFs were prepared from hearts of 1- to 3-day-old Sprague-Dawley rats, finely minced, and placed in 0.08% trypsin at 37°C for 5 minutes 5 times. The resuspension was plated in culture flasks with Dulbecco's modified Eagle's medium (Gibco, Grand Island, NY) containing 10% fetal bovine serum (BioInd, Beit HaEmek, Israel) in humidified air with 5% CO_2 at 37°C. Cells were cultivated to passage 3 to 9. CF transfection involved the miR-26a mimic (JTS Scientific, China) or the miR-26a inhibitor (JTS Scientific, Shanghai, China), or a corresponding negative control (NC) according to the manufacturer's instructions. After 24-hour transfection, cells were treated with AngII (10^{-7} mol/L for 24 hours).

CCK-8 Assay

Culture medium of cells was discarded and cells were washed with PBS, then added with 10-µL CCK8 (Wanleibio, Shenyang, China), and incubated for 1 hour under 5% CO_2 at 37°C. A microplate reader (BioTek, Winooski, VT) was used to detect the optical density at 450 nm, which represents cell proliferation.

Cell Cycle Assay

Each group of cells was washed twice with PBS; cells were harvested by centrifugation and resuspended in PBS, then fixed with 70% ethanol at 4°C for 2 hours. To remove ethanol, cells were washed twice in ice-cold PBS, then resuspended in a solution containing 100-µL RNase A and 500-µL propidium iodide (Wanleibio) at 37°C for 30 minutes in the dark. Cell cycle was detected by flow cytometry (NovoCyte; Acea Biosciences, San Diego, CA).

Quantitative Real-Time Polymerase Chain Reaction

Total RNA was extracted from plasma, heart tissues, and CFs by using Trizol reagent (Thermo Fisher Scientific, Waltham, USA) and digested with RNase. cDNA was synthesized by using an miRNA Reverse Transcription System kit (TaKaRa Bio, Otsu, Japan) and 2×SYBR real-time PCR premixture (Bioteke Corp, Beijing, China) for quantitative real-time polymerase chain reaction (qPCR). Real-time PCR involved using the StepOnePLus Real-Time PCR System (Thermo Fisher Scientific). The gene-specific primer sequences (TaKaRa Bio) are shown in Table S1, and conditions for amplification are shown in Table S2. The relative expression was calculated by the $2^{-\Delta\Delta Ct}$ method. U6 and β-actin were the internal references, respectively.

Western Blot Analysis

The middle segment of the left ventricle was collected, cut into 0.5×0.5-cm segments, washed clean with clear water, dried with filter paper, placed in sterile tubes, and stored in liquid nitrogen quickly. Frozen tissue and CFs were homogenized in liquid nitrogen, then the homogenate was lysed in radio immunoprecipitation assay buffer lysate (WB009A; Hat Biotechnology, Xi'an, China) and phenylmethanesulfonyl fluoride (WB009C, Hat Biotechnology) on ice for 10 minutes.

After centrifugation at 12 000g for 10 minutes at 4°C, the supernatant was collected and quantified with bicinchoninic acid before being degenerated by mixing with SDS-PAGE sample loading buffer, 5 times (P0015L; Beyotime Biotechnology, Jiangsu, China) at 100°C for 5 minutes. Equal amounts of protein were loaded and separated by 10% SDS-PAGE. Then proteins were transferred to polyvinylidene difluoride membranes by electroblotting. Membranes were blocked with 5% skimmed milk for at least 1 hour at room temperature, then incubated with specific primary antibodies against Smad3 (ab40854; Abcam, Cambridge, UK; 1:1000 dilution), Smad4 (ab40759, Abcam; 1:1000 dilution), phospho-Smad3 (ab193297, Abcam; 1:500 dilution), matrix metalloproteinase 2 (MMP2; ab92536, Abcam; 1:1000 dilution), connective tissue growth factor (CTGF; ab6992, Abcam; 1:1000 dilution), transforming growth factor βRI (TGFβRI; ab31013, Abcam; 1:1000 dilution); collagen I (Col I; WL0088, Wanleibio; 1:500 dilution), Col III (WL0318, Wanleibio; 1:500 dilution); enhancer of zeste homolog 2 (EZH2; 5246; Cell Signaling Technology, Beverly, MA; 1:500 dilution); p21 (ab109199, Abcam; 1:500 dilution), β-actin (WL01372, Wanleibio; 1:500 dilution), GAPDH (AF7021, Affinity Biosciences, Cincinnati, OH; 1:1000 dilution) overnight at 4°C. After washing with tris-buffered saline and polysorbate 20 three times (each for 5 minutes), membranes were incubated for 1 hour with goat anti-rabbit IgG antibody (EK020, Zhuangzhi Biotech, Xi'an, China; 1:5000 dilution) at room temperature, then rinsed 3 times with tris-buffered saline and polysorbate 20 (each for 10 minutes). The immunoreactive bands were visualized by using a potent ECL (enhanced chemiluminescent) kit (KF001; Affinity Biosciences) by using the Gene Company Ltd. imaging system (Chai Wan, Hong Kong, China). The result was presented as the ratio of target proteins to GAPDH level.

Luciferase Reporter Assay

The mutant-type (MuT) 3′-UTR of EZH2, CTGF, and Smad4 was constructed. The wild-type (WT) and MuT 3′-UTR of EZH2, CTGF, and Smad4 were inserted into pMIRGLO vectors (Promega, San Luis Obispo, CA). The miR-26a mimic, miR-NC, WT 3′-UTR and MuT 3′-UTR of EZH2, CTGF, and Smad4 vector were cotransfected into HEK293T (Wanleibio) cells. After 48 hours, cells were lysed, and luciferase activity was determined by using a luciferase assay kit (Promega) and multifunction microplate reader (M200Pro, TECAN, Männedorf, Switzerland).

Statistical Analysis

GraphPad Prism 6 software (GraphPad Software, Inc, La Jolla, CA) was used to analyze data. SPSS 21.0 (SPSS, Inc, Chicago, IL) was used for normality test. Data are expressed as mean±SD. To determine differences between groups with 1 factor, data were tested using Student t test for 2-group comparison with normally distributed values, and 1-way ANOVA followed by Tukey multiple comparisons test for multiple group comparisons. To determine differences between groups with multiple factors, data were tested using 2-way ANOVA followed by Bonferroni post test. For staining, analyses were performed using a nonparametric Mann–Whitney U test or Kruskal–Wallis test. Differences were considered significant at $P<0.05$.

RESULTS

## miR-26a Was Linked to Hypertension and MF

We examined the plasma and myocardial levels of miR-26a in both SHRs and WKYs at 2 different ages. miR-26a levels did not differ between 8- and 16-week-old WKYs (Figure 1B and 1C), which suggests that the expression of miR-26a was not affected by age. Nonetheless, plasma and myocardial miR-26a levels were significantly lower in SHRs than WKYs, and miR-26a level in plasma and myocardium was markedly decreased in SHRs at 16 weeks versus 8 weeks (Figure 1B and 1C). In addition, SBP in SHRs was higher at 16 than 8 weeks (Figure 1A). These results suggest that the plasma and myocardial miR-26a levels might be associated with BP in vivo.

We also observed hematoxylin and eosin and Masson's staining in myocardial tissues of miR-26a⁺/⁻ mice (miR-26a⁺/⁻) and WT miR-26a⁺/⁺ mouse littermates. Histopathological examination showed no abnormalities in cardiomyocytes in the WT group. In the miR-26a⁺/⁻ group, myocardial fiber rupture was obvious. Masson's staining showed that WT mice had only a small amount of collagen in myocardium, whereas a great amount of blue collagen occupied myocardial tissue in miR-26a⁺/⁻ mice and the collagen volume fraction was significantly increased (Figure 1D and 1E). The miR-26a level was significantly lower in miR-26a⁺/⁻ mice than in WT mice (Figure 1F). These results indicated that MF was inversely associated with the miR-26a level in myocardial tissue.

miR-26a Regulates Blood Pressure in Rats With Hypertension

For the purpose of investigating the role of miR-26a in hypertension, rAAV vectors were constructed to mediate the functional acquisition of miR-26a in a hypertensive animal model. The results indicated that rAAV-miR-26a transfection significantly increased the expression of miR-26a (Figure 2A and 2B).
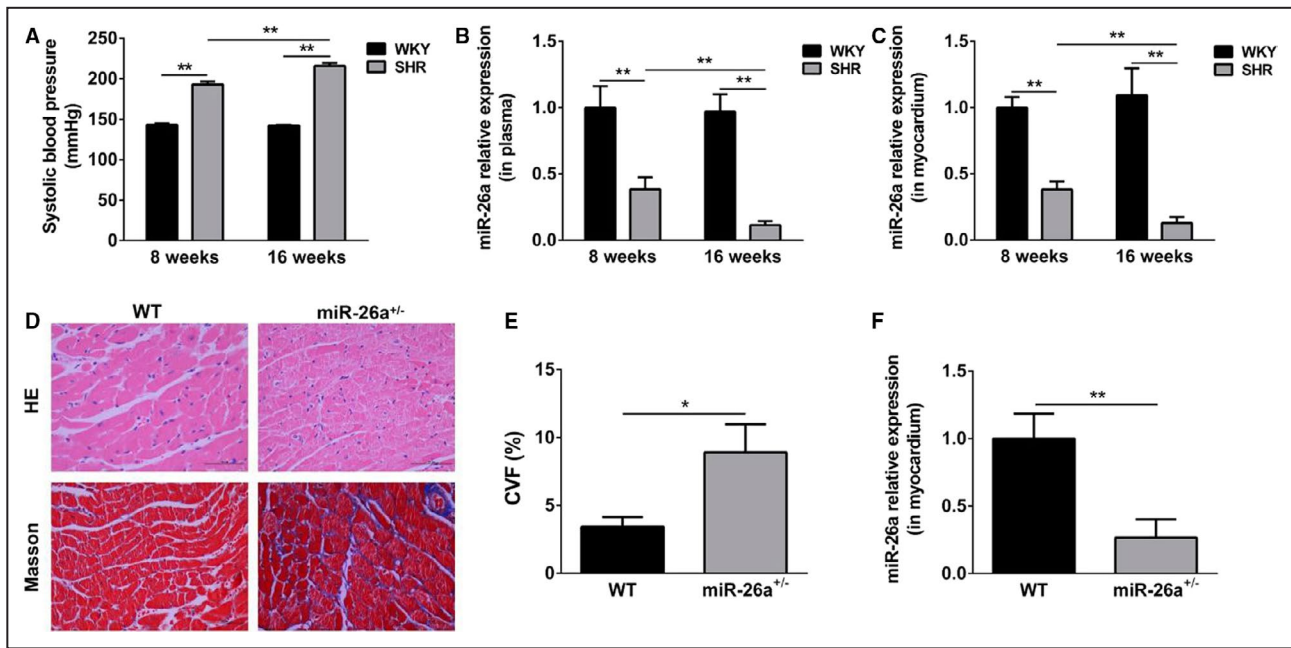
Figure 1. Expression patterns of miR-26a in spontaneously hypertensive rats (SHRs) and miR-26a⁺/⁻ mice.

A–C, 8- and 16-week-old male Wistar-Kyoto rats (WKYs) and spontaneously hypertensive rats (SHRs). A, Systolic blood pressure in WKYs and SHRs. B and C, microRNA-26a (miR-26a) relative expression in plasma (B) and myocardium (C) in WKYs and SHRs. Data are mean±SD (n=6 per group); **$P<0.01$. D through F, 18- to 20-week-old male miR-26a⁺/⁻ mice and wild-type (WT) miR-26a⁺/⁺ mouse littermates. D, Representative images of hematoxylin and eosin (HE) and Masson's staining in myocardial tissues from miR-26a⁺/⁻ and WT mice. Scale bars, 50 μm. E, Collagen volume fraction (CVF) of myocardium with Masson's staining. F, Relative expression of miR-26a in myocardial tissue of miR-26a⁺/⁻ and WT mice. Data are mean±SD (n=4 per group); *$P<0.05$; **$P<0.01$. Statistical significance was determined using Student t test for 2-group comparison, 1-way ANOVA followed by Tukey multiple comparisons test for multiple group comparisons and Mann–Whitney U test for Masson's staining analyses.

At the beginning of the experiment, BP did not differ significantly among the SHR groups ($P>0.05$). SBP of SHRs not treated with rAAV-miR-26a increased from a baseline of 194±7.4 mm Hg (at 8 weeks) to a peak of 208±7 mm Hg (at 11 weeks) and remained at a high level, whereas that of control WKYs was always maintained at a normal level of 142±3.7 mm Hg. However, rAAV-miR-26a treatment significantly prevented BP from elevating in SHRs. After 3 weeks of injection, SBP was significantly higher in vector (rAAV-GFP) and vehicle (SHR-Ctrl) controls than rAAV-miR-26a–treated animals ($P<0.05$, respectively), with no significant difference between the 2 SHR groups ($P>0.05$; Figure 2C).

## miR-26a has a Protective Effect on Hypertension-Induced Myocardial Fibrotic Remodeling

Histopathological examination showed no obvious abnormality in cardiac muscle cells in the WKY group. In SHR vector- and vehicle-treated controls, cardiomyocytes were disordered, and nuclei were deeply stained; myocardial fibers were broken, and interstitial fibrosis was proliferated. The rAAV-miR-26a–treated group showed a significant improvement in cardiomyocyte morphology and arrangement (Figure 3A).

Cardiac fibrosis examined by Masson's trichrome staining revealed significantly decreased area of MF in rAAV-miR-26a–treated animals as compared with SHR vector- and vehicle-treated controls ($P<0.05$, respectively), but increased as compared with the WKY group ($P<0.05$; Figure 3A and 3B).

To further determine the effect of miR-26a in the amelioration of tissue fibrosis in SHRs, we examined the fibrogenetic protein levels of MMP2, CTGF, TGFβRI, Smad3, Smad4, and phospho-Smad3. The expressions of MMP2, CTGF, TGFβRI, phospho-Smad3, and Smad4 were notably reduced in the WKY group as compared with the other 3 groups ($P<0.05$). The above-mentioned protein levels were also significantly decreased in rAAV-miR-26a–treated rats as compared with vector- and vehicle-treated controls ($P<0.05$), but were higher than in the WKY group ($P<0.05$). The protein level of Smad3 in each group was similar ($P>0.05$; Figure 3C). These observations suggest that rAAV-miR-26a significantly attenuated MF in SHRs.

miR-26a Inhibited AngII-Induced Extracellular Matrix Release From CFs

Figure 4A shows that AngII could inhibit the expression of miR-26a in CFs. When the miR-26a mimic and
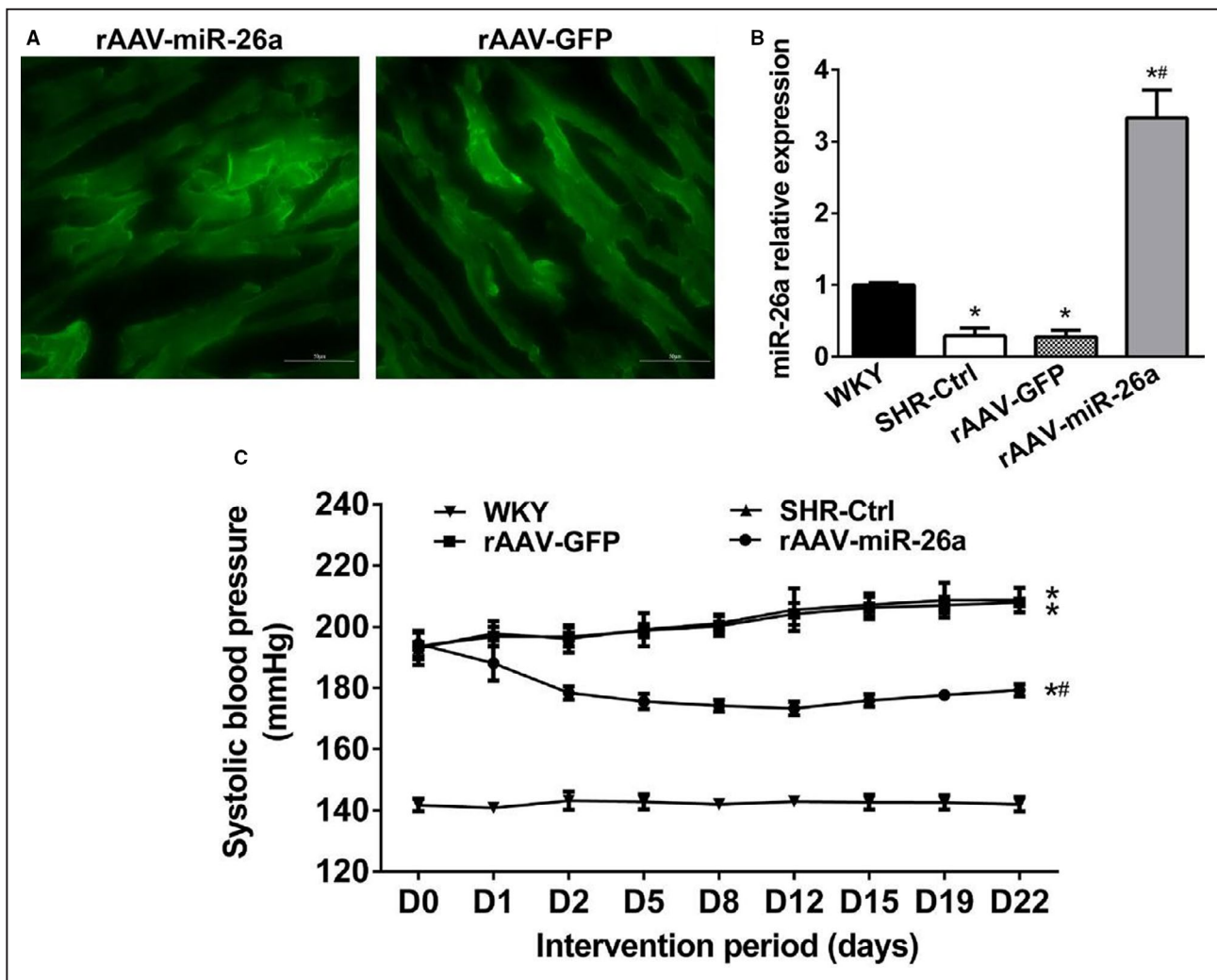
**Figure 2.   microRNA-26a (miR-26a) regulates blood pressure in spontaneously hypertensive rats (SHRs).**
SHRs (n=8 per group) were injected by tail vein with recombinant adeno-associated virus (rAAV-) miR-26a, rAAV-GFP, or saline, and WKYs (n=6) were injected by tail vein with saline as normal controls. **A**, Viral fluorescence in myocardium after administration with various virus-expressing vectors. Scale bars, 50 μm. **B**, Relative mRNA levels of miR-26a in myocardium in rats. **C**, Systolic blood pressure of each group before and after the intervention. Data are mean±SD. *$P<0.05$ vs WKY, #$P<0.05$ vs rAAV-GFP and SHR-Ctrl. Statistical significance was determined using one-way ANOVA followed by Tukey multiple comparisons test.

inhibitor were transfected into AngII-induced CFs, the results showed high-transfection efficiency. To define the role of miR-26a in AngII-triggered profibrotic response, we assessed the efficacy of miR-26a mimic and inhibitor transfection in CFs stimulated with AngII. The mRNA and protein levels of Col I, Col III, MMP2, and TGFβRI were increased in cells treated with AngII as compared with unstimulated cells. miR-26a mimic transfection of CFs in the presence of AngII significantly attenuated the expression of Col I, Col III, MMP2, and TGFβRI, whereas miR-26a inhibitor transfection of CFs in the presence of AngII further increased the expression of these fibrotic genes as compared with AngII-treated cells alone (Figure 4B through 4D). Together, our results illustrate a strong negative association between miR-26a and MF.

miR-26a Protects Myocardium From Hypertension-Induced Cell Proliferation

One of the pathological bases of MF is cell proliferation. The proliferation index of myocardial stromal fibroblasts was defined as the proportion of Ki-67+ nuclei per total nuclei sample. The proliferation rate was significantly lower for rAAV-miR-26a–treated animals than SHR vector- and vehicle-treated controls ($P<0.05$), but higher than the WKY group ($P<0.05$; Figure 5A and 5B).

In vitro, the CF proliferation level was measured by CCK-8 assay and flow cytometry. miR-26a mimic treatment significantly inhibited the proliferation rate and increased the proportion of cells in the G1 phase of CFs as compared with AngII, mimic NC (NC)+AngII, and inhibitor NC+AngII groups ($P<0.05$; Figure 6A and 6B). The CCK-8 assay also showed that the miR-26a mimic
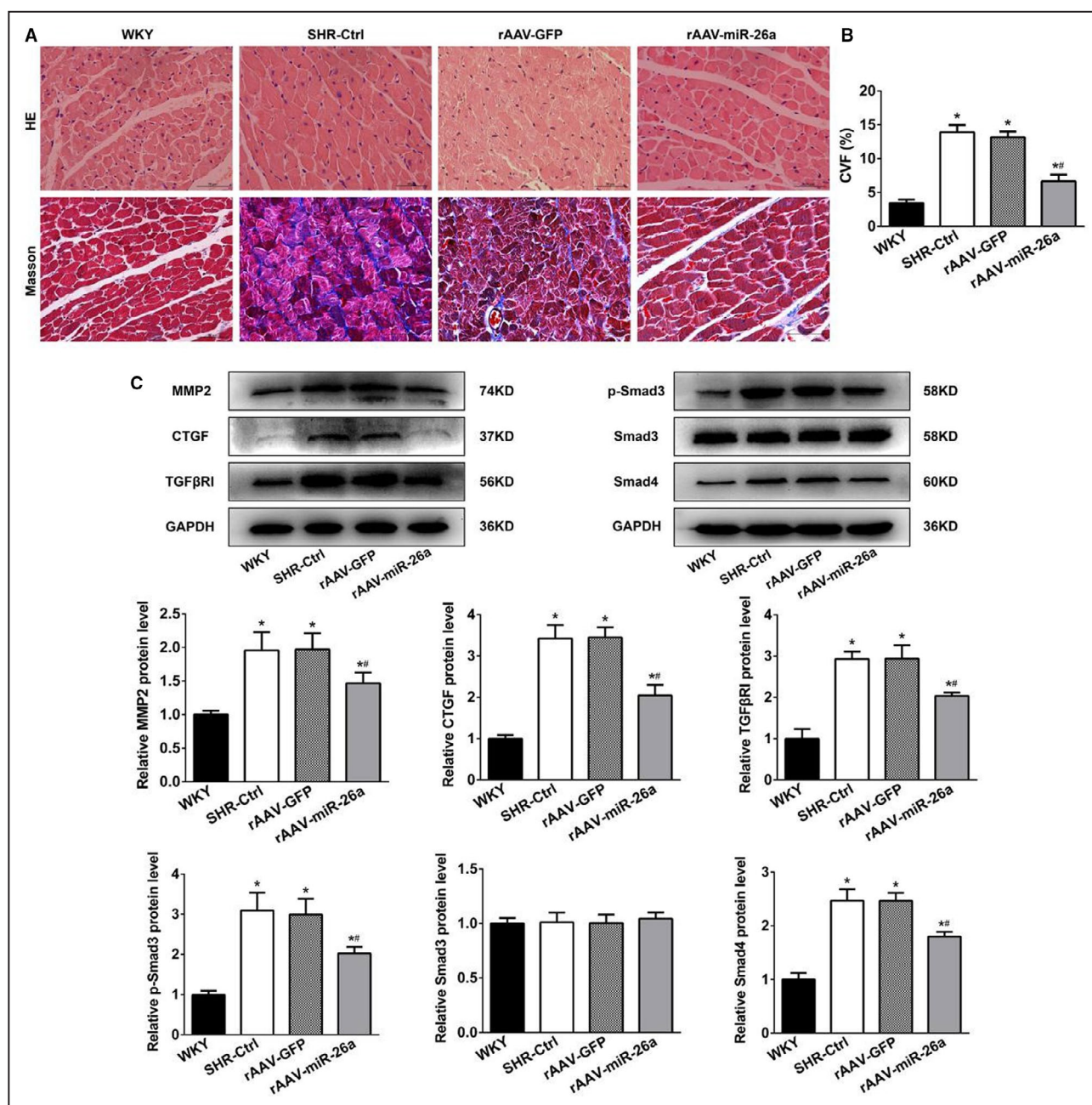
Figure 3. microRNA-26a (miR-26a) has a protective effect on hypertensive myocardial fibrosis in spontaneously hypertensive rats (SHRs).
Myocardial morphological analysis and relative expression of fibrotic indicators in SHRs and Wistar-Kyoto rats (WKYs) with different treatment groups. **A**, Representative images of morphological staining in myocardial tissues from WKYs and SHRs, Scale bars, 50 μm. **B**, Quantification of myocardial fibrosis. **C**, Relative protein levels of MMP2, CTGF, TGFβRI, Smad3, Smad4, and p-Smad3 in myocardium from WKYs and SHRs with different treatments. Data represent the end of the experiment, Data are mean±SD (n≥3). *$P<0.05$ vs WKY, #$P<0.05$ vs rAAV-GFP and SHR-Ctrl. Statistical significance was determined using 1-way ANOVA with Tukey test and Masson's staining analysis was determined by Kruskal–Wallis test. CTGF indicates connective tissue growth factor; CVF, collagen volume fraction; MMP2, matrix metalloproteinase 2; p-Smad3, phospho-Smad3; and TGFβRI, transforming growth factor-β receptor I.

promoted AngII-induced CF proliferation ($P<0.05$; Figure 6C). These results suggest that miR-26a inhibited cell proliferation in CFs.

To further determine the mechanism by which miR-26a regulated cell proliferation, we evaluated the EZH2 and p21 protein level in the myocardium of

SHRs and WKYs. Treatment with rAAV-miR-26a effectively decreased EZH2 protein expression ($P<0.05$) and increased p21 protein expression as compared with vector and vehicle treatment ($P<0.05$). However, rAAV-miR-26a treatment only promoted partial reversal of EZH2 and p21 protein levels in SHRs as compared
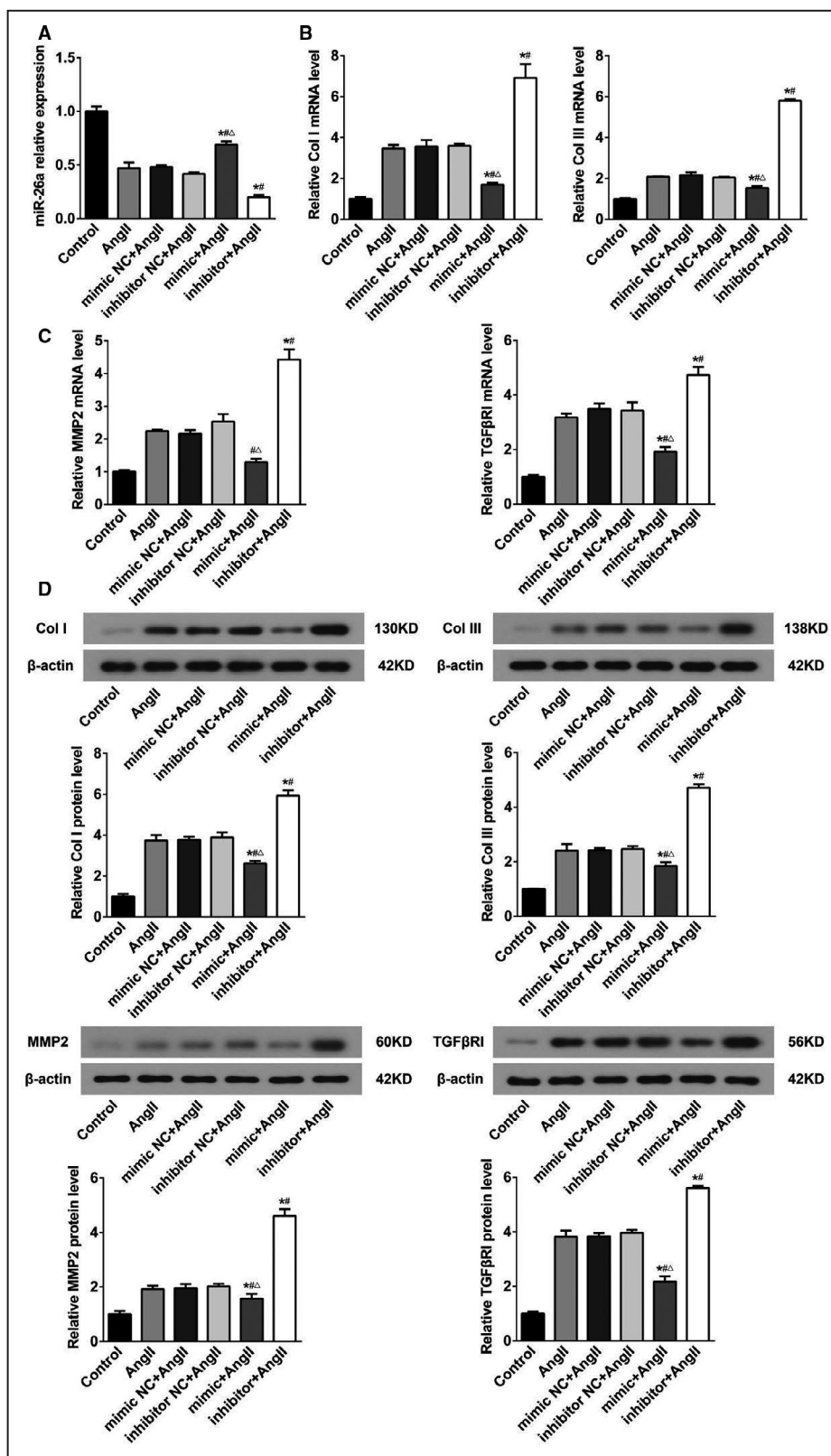
with the WKY group (*P*<0.05; Figure 5C). These results suggest that miR-26a inhibition of hypertension-induced cell proliferation may be achieved by regulating proliferation-related genes EZH2 and p21.

EZH2, CTGF, and Smad4 Are Physiological Targets of miR-26a

Among AngII-treated groups, the protein levels of EZH2, CTGF, and Smad4 were the highest in the

Figure 4.   microRNA-26a (miR-26a) inhibited AngII-induced extracellular matrix release from cardiac fibroblasts (CFs).
AngII-induced CFs were transfected with miR-26a mimic, inhibitor, or corresponding NC. The control group was a blank control without any treatment, and the AngII group received AngII only. **A,** Relative miR-26a expression in different treatment groups in CFs. B and C, Relative mRNA expression of Col I, Col III, MMP2, and TGFβRI in CFs. D, Relative protein levels of TGFβRI, MMP2, Col I, and Col III in CFs from different treatment groups. Data are mean±SD (n=3). *$P<0.05$ vs control, #$P<0.05$ vs AngII, mimic NC+AngII and inhibitor NC+AngII, △$P<0.05$ vs inhibitor+AngII. Statistical significance was determined using 1-way ANOVA with Tukey test. AngII indicates angiotensin II; Col I, Col III, collagen I, collagen III; MMP2, matrix metalloproteinase 2; NC, negative control; and TGFβRI, transforming growth factor-β receptor I.

inhibitor group and the lowest in the mimic group ($P<0.05$), with no significant difference among the AngII, mimic NC+AngII, and inhibitor NC+AngII groups ($P>0.05$; Figure 7A, 7E, and 7I). The relative mRNA expression of EZH2, CTGF, and Smad4 was consistent with the protein expression (Figure 7C, 7G, and 7K),

so miR-26a downregulated the expression of EZH2, CTGF, and Smad4.

Bioinformatics analysis using Targetscan (www. targetscan.org) and miRanda (www.microRNA.org) indicated EZH2, CTGF, and Smad4 as potential target genes of miR-26a (Figure 7B, 7F, and 7J). Using a
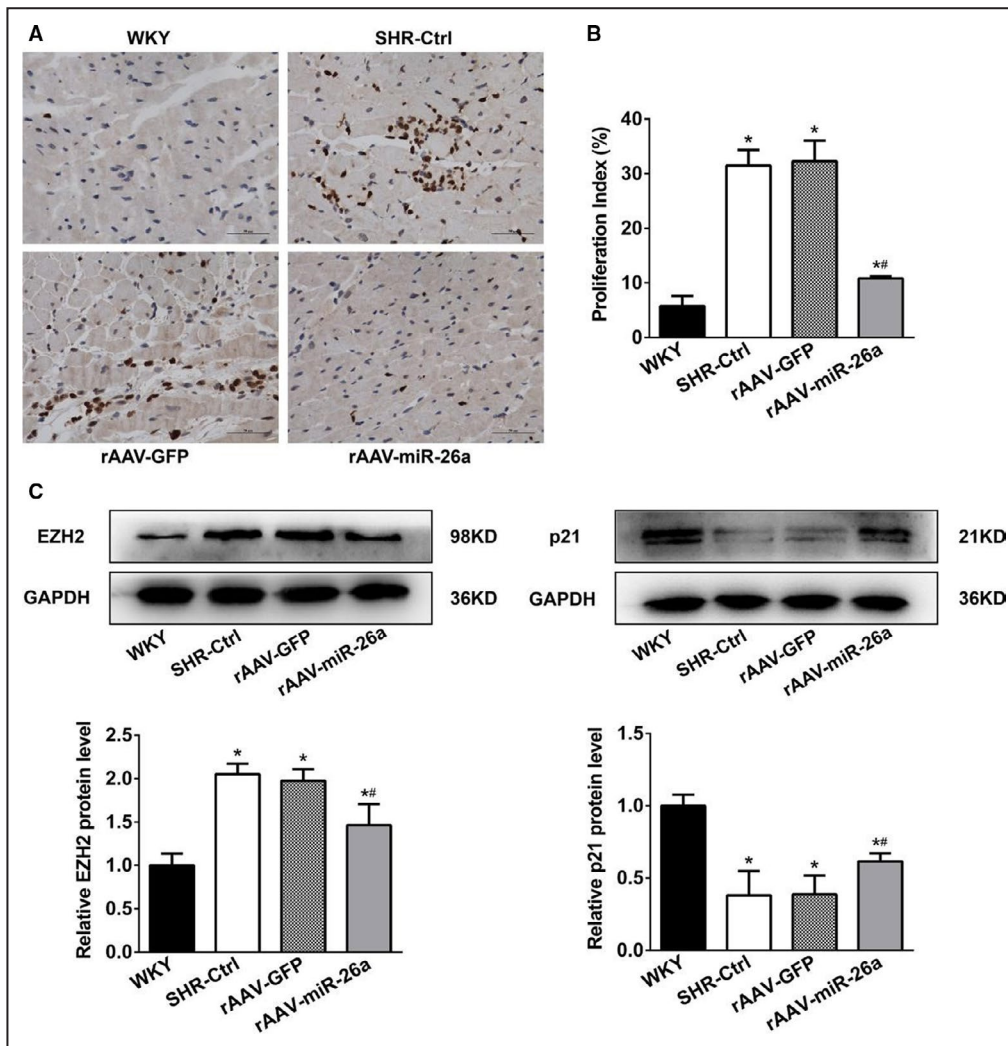
Figure 5.   microRNA-26a (miR-26a) protects myocardium from cell proliferation in spontaneously hypertensive rat (SHRs).
Myocardial stromal fibroblasts proliferation index and related protein expression in SHRs and Wistar-Kyoto rats (WKYs) with different treatments. **A,** The expression of Ki-67 in myocardial stromal fibroblasts detected by immunohistochemistry. Scale bars, 50 µm. **B,** Myocardial stromal fibroblast proliferation index defined as the proportion of Ki-67+ nuclei per total nuclei sample (5 rats ×10 scope field count in each group). **C,** Relative protein levels of EZH2 and p21 in myocardium from WKYs and SHRs with different treatments. Data are mean±SD (n≥3). *$P<0.05$ vs WKY, #$P<0.05$ vs rAAV-GFP and SHR-Ctrl. Statistical significance was determined using 1-way ANOVA with Tukey test. EZH2 indicates enhancer of zeste homolog 2.
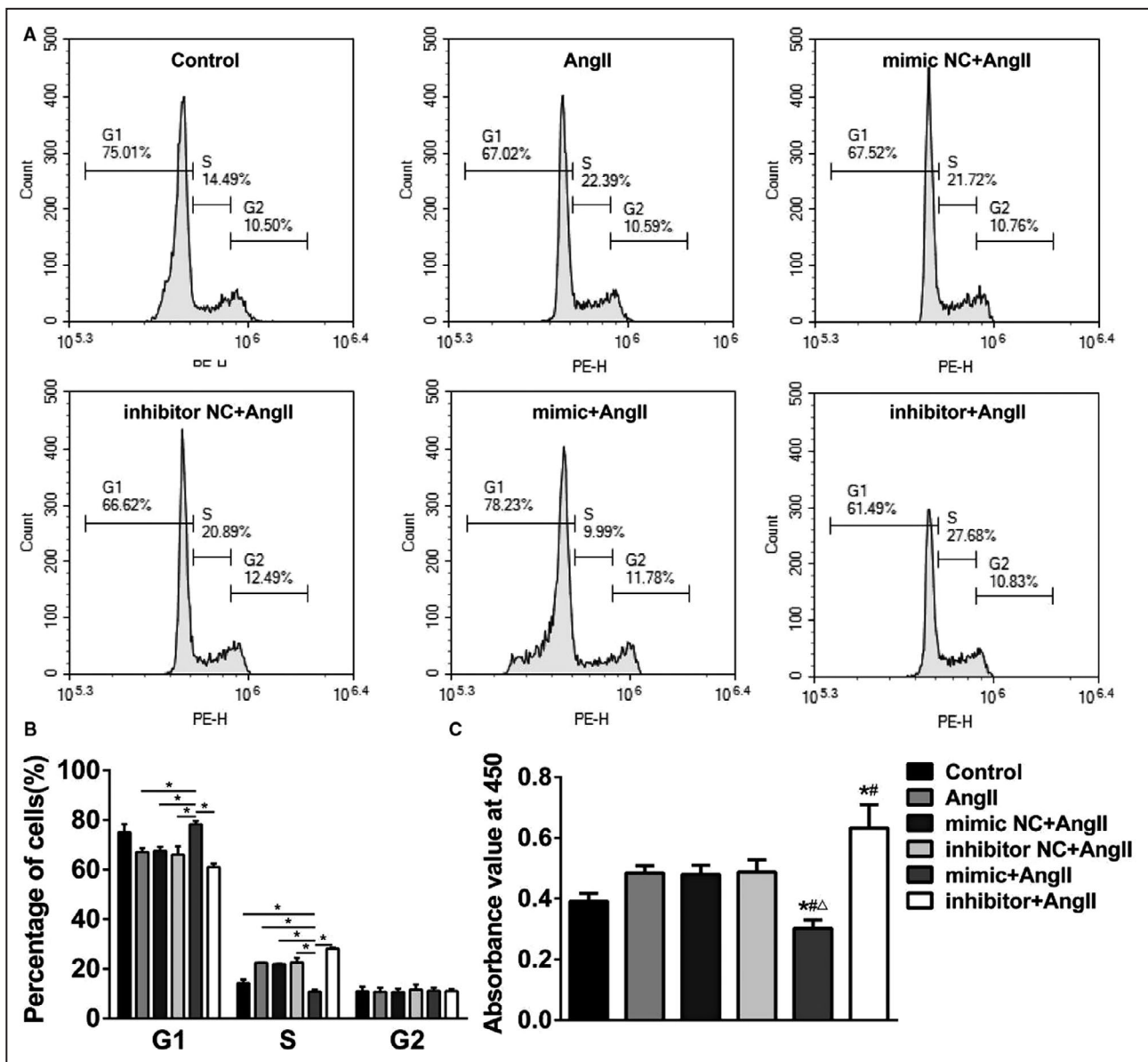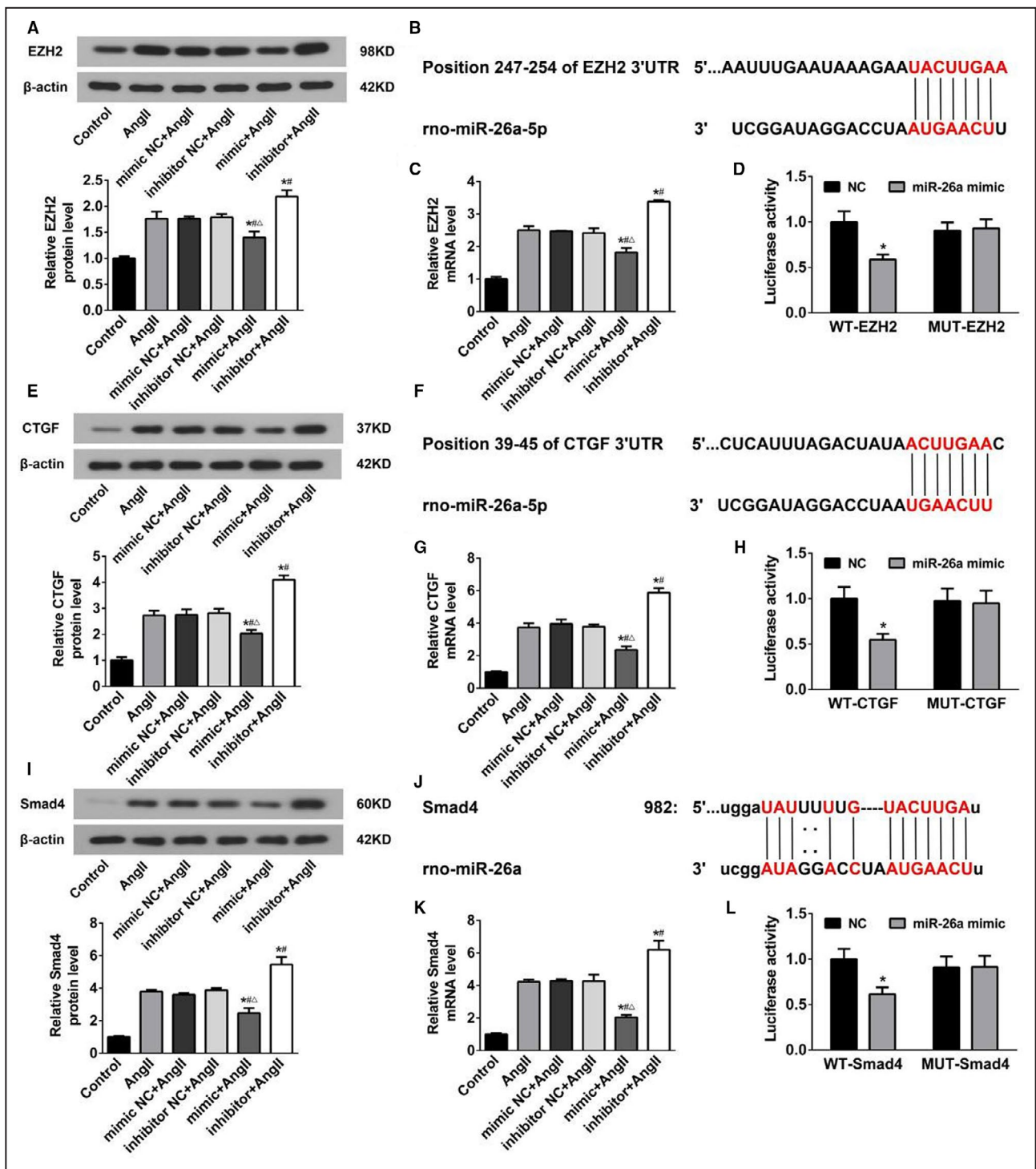
Figure 6. microRNA-26a (MiR-26a) inhibited AngII-induced proliferation of cardiac fibroblasts (CFs).
A and **B**, Comparisons of cell cycles among groups in CFs detected by propidium iodide (PI) single staining. **A**, Cell cycle in each group. **B**, Proportion of cells in the G1, S, and G2 phases in each group. Data are mean±SD (n=3), *P<0.05. (**C**) CCK-8 assays of the effect of miR-26a on growth of CFs. Data are from 5 independent experiments, with at least 3 replicates in each independent experiment. *P<0.05 vs control, #P<0.05 vs AngII, mimic NC+AngII and inhibitor NC+AngII, △P<0.05 vs inhibitor+AngII. Statistical significance was determined using 1-way ANOVA with Tukey test. AngII indicates angiotensin II, and NC, negative control.

reporter construct with the putative 3′-UTR miR-26a binding site of EZH2, CTGF, and Smad4 downstream of the luciferase gene, we found that miR-26a reduced luciferase activity, which provides experimental validation of EZH2, CTGF, and Smad4 as targets for miR-26a. Accordingly, after mutation of the binding site, luciferase activity could not be altered, which confirms that the binding of miR-26a to their 3′-UTR sites was necessary for silencing EZH2, CTGF, and Smad4 (Figure 7D, 7H, and 7L).

DISCUSSION

In this study, we found that miR-26a was involved in hypertension and MF. MiR-26a significantly prevented BP elevation and inhibited MF in vivo and AngII-induced fibrogenesis in CFs. Furthermore, we revealed that miR-26a reduced collagen, extracellular matrix (ECM) deposition by directly targeting CTGF, and miR-26a inhibited TGFβ/Smad signal pathway by directly targeting Smad4. Additionally, miR-26a inhibited CF

Figure 7. EZH2, CTGF, and Smad4 are physiological targets of microRNA-26a (miR-26a).
MiR-26a inhibits EZH2, CTGF and Smad4 expression and targets the 3′ UTR of EZH2, CTGF and Smad4. **A**, **E**, and **I**, Relative protein levels of EZH2, CTGF and Smad4 after the introduction of miR-26a into CFs. **C**, **G**, and **K**, Relative mRNA levels of EZH2, CTGF and Smad4 in CFs. Data are mean±SD (n=3). *$P<0.05$ vs control, #$P<0.05$ vs AngII, mimic NC+AngII and inhibitor NC+AngII, △$P<0.05$ vs inhibitor+AngII. Statistical significance was determined using 1-way ANOVA with Tukey test. **B**, **F**, and **J**, Prediction of miR-26a targets was conducted in silico and EZH2, CTGF, and Smad4 were selected as candidates. **D**, **H**, and **L**, Luciferase reporter gene detection results. Luciferase activities were analyzed by dual-luciferase reporter assay. Data are mean±SD (n=3), *$P<0.05$ vs WT NC group and MUT miR-26a mimic group. Statistical significance was determined using 2-way ANOVA followed by Bonferroni posttest. AngII indicates angiotensin II; CTGF, connective tissue growth factor; EZH2, enhancer of zeste homolog 2; MUT, mutation type; NC, negative control; and WT, wild type.

proliferation by the EZH2/p21 pathway. Our study reveals a novel role for miR-26a in BP control and hypertensive MF and provides a possible treatment strategy for miR-26a in alleviating and reversing hypertensive MF (Figure 8).

MF induced by hypertension contributes to structural and functional damage to the myocardium, which can adversely affect the clinical outcomes in patients with hypertension.[17] MF is characterized by excess deposition of ECM and proliferation of CFs.[18,19] MiRNAs are perceived as novel therapeutic strategies in cardiovascular disease because of their crucial roles in various cardiovascular systems,[20–22] and miR-26a plays an important role in antifibrosis and inhibition of cell proliferation.[23,24] In the present study, we evaluated the role and mechanism of miR-26a in controlling hypertensive MF. We used hypertensive animal models and miR-26a knockout mice to demonstrate that miR-26a is involved in hypertension and MF. MiR-26a overexpression significantly prevented BP elevation and protected the

myocardium against fibrosis in vivo. Similarly, miR-26a downregulated the expression of AngII-induced fibrotic factors in vitro. In addition, we confirmed that miR-26a inhibited excessive deposition of ECM and CF proliferation both in vitro and in vivo. Therefore, miR-26a is a protective factor for hypertensive MF.

MiR-26a can regulate the expression of multiple genes for antifibrotic effects.[25,26] The above-noted effects of miR-26a might be related to the regulation of downstream molecules. CTGF, a newly defined cell factor that takes part in regulating the secretion of ECM by fibroblasts, has important roles in the fibrosis of various organs, including the liver, kidney, and heart ventricles.[27] Inhibiting the expression of CTGF protein may prevent fibrosis.[28,29] Smad4 is the common partner for all Smads and interacts with other Smads to form stable heteromultimers, which are translocated into the nucleus and regulate transcription of target genes. As a pivotal protein in the signal pathway, Smad4 interacts with other Smad proteins and serves as the key link in
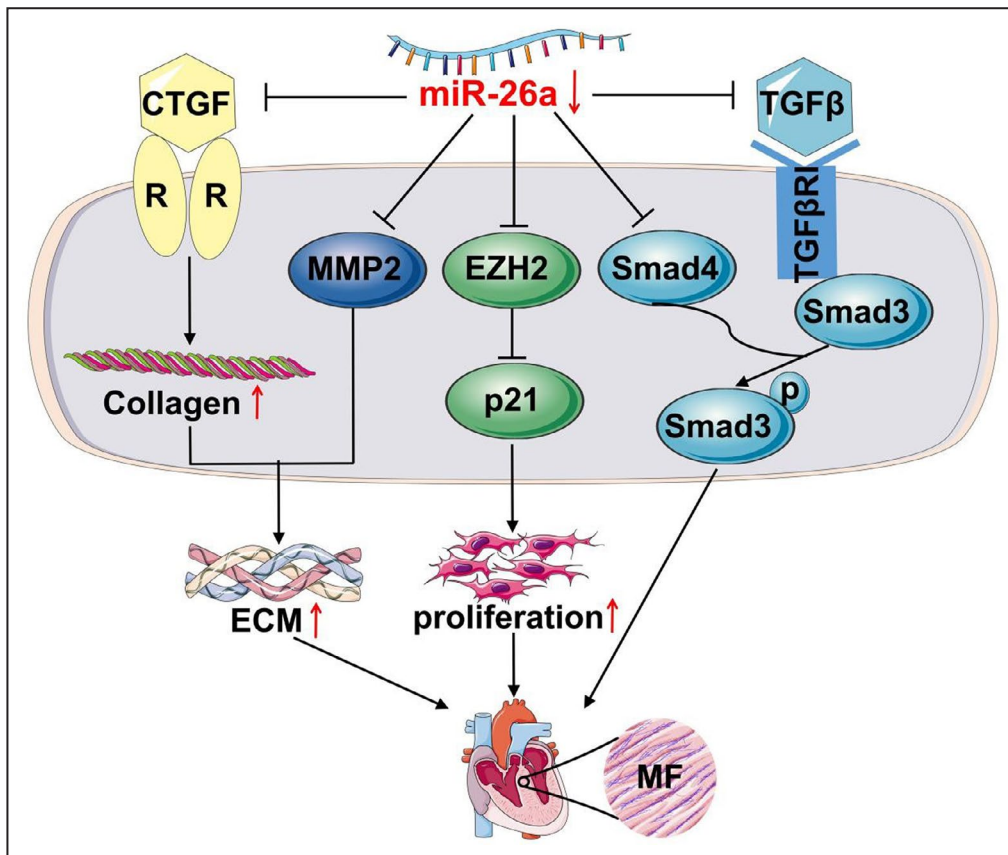
Figure 8.   Proposed model for the role of microRNA-26a (miR-26a) in hypertensive MF.
Reduced miR-26a level increases CTGF and MMP2 levels, leading to production of collagens and ECM. Downregulation of miR-26a upregulates the expression of EZH2 and downregulates that of p21, leading to CF proliferation. Excessive deposition of ECM and CF proliferation are the main pathological basis of myocardial fibrosis. Meanwhile, downregulation of miR-26a upregulates Smad4, which promotes fibrosis regulated by the TGFβ/Smad signal pathway. CTGF indicates connective tissue growth factor; ECM, extracellular matrix; EZH2, enhancer of zeste homolog 2; MF, myocardial fibrosis; MMP2, matrix metalloproteinase 2; p, phosphorylation; R, receptor; and TGF, transforming growth factor.

the signal transduction pathway of the TGFβ superfamily to regulate downstream effectors or crosstalk pathways, thereby playing a pivotal role in the signaling process. Specific silencing of Smad4 can inhibit fibrosis regulated by the TGFβ/Smad signal pathway and block activation of the pathway. Also, Smad4 silencing inhibits fibrosis.[30] Therefore, Smad4 is closely related to fibrosis. Our luciferase reporter gene detection system and in vitro experiments confirmed that CTGF and Smad4 are the target genes of miR-26a. Reduced expression of CTGF induced collagen production. Loss inhibition of Smad4 activated the TGFβ/Smad signal pathway and promoted fibrosis regulated by the TGFβ/Smad pathway, which exacerbated the development of MF. Previous research showed that miR-26a negatively regulates the expression of other ECM proteins involved in fibrosis, including MMP2, and mitigates collagen deposition.[16,31] Our study indicated that downregulation of miR-26a could increase the expression of MMP2, Col I, and Col III. miR-26a may protect the myocardium against fibrosis, directly mediated via CTGF and Smad4. Furthermore, the antifibrotic effects of miR-26a could be achieved by inhibiting the expression of other fibrotic genes.

We also found that the EZH2 was the direct target of miR-26a and that miR-26a can inhibit EZH2 expression. EZH2 could regulate gene expression in mature cardiomyocytes, and myocardium hypertrophy is associated with the release of EZH2.[32,33] Suppressing EZH2 enhances the differentiation of CFs into beating cardiomyocytes.[34] Also, EZH2/p21 is a crucial signaling pathway that could regulate cell proliferation.[35,36] In our study, we confirmed that decreased expression of miR-26a downregulated the expression of EZH2 and upregulated that of p21. Thus, the EZH2/p21 pathway may be a related signal pathway regulated by miR-26a during CF proliferation.

In summary, miR-26a may be a protective gene for hypertensive MF. Downregulation of miR-26a led to excessive deposition of ECM and CF proliferation, thereby resulting in MF. miR-26a might be an important therapeutic target to prevent and control hypertensive MF.

Limitations and Prospects

Our experiment only focused on hypertensive MF. We revealed the therapeutic target and molecular mechanism of miR-26a on hypertensive MF, but did not study whether this target has a protective effect on nonhypertensive MF, which can be a future study. Meanwhile, we found that miR-26a may be involved in hypertension. However, we have not monitored the dynamic expression changes of miR-26a in SHR myocardium after rAAV-miR-26a injection, so it is difficult to confirm that miR-26a has a direct antihypertensive effect. Our study also identified 3 targets for miR-26a, but we did not study whether overexpression of the target proteins block or reduce the protective effects of miR-26a. We will further validate the role of EZH2, CTGF, and Smad4 as specific targets of miR-26a in future studies.

REFERENCES

1. Cai G, Zhang X, Weng W, Shi G, Xue S, Zhang B. Associations between PPARG polymorphisms and the risk of essential hypertension. *PLoS One*. 2017;12:e0181644.
2. Huang J, Yan ZN, Rui YF, Fan L, Shen D, Chen DL. Left ventricular systolic function changes in primary hypertension patients detected by the strain of different myocardium layers. *Medicine (Baltimore)*. 2016;95:e2440.
3. Verjans R, Peters T, Beaumont FJ, van Leeuwen R, van Herwaarden T, Verhesen W, Munts C, Bijnen M, Henkens M, Diez J, et al. MicroRNA-221/222 family counteracts myocardial fibrosis in pressure overload-induced heart failure. *Hypertension*. 2018;71:280–288.
4. Drazner MH. The progression of hypertensive heart disease. *Circulation*. 2011;123:327–334.
5. Verdecchia P, Porcellati C, Reboldi G, Gattobigio R, Borgioni C, Pearson TA, Ambrosio G. Left ventricular hypertrophy as an independent predictor of acute cerebrovascular events in essential hypertension. *Circulation*. 2001;104:2039–2044.
6. Quintana-Villamandos B, Gomez de Diego JJ, Delgado-Martos MJ, Munoz-Valverde D, Soto-Montenegro ML, Desco M, Delgado-Baeza E. Dronedarone produces early regression of myocardial remodelling in structural heart disease. *PLoS One*. 2017;12:e0188442.
7. Wang F, Fang Q, Chen C, Zhou L, Li H, Yin Z, Wang Y, Zhao CX, Xiao X, Wang DW. Recombinant adeno-associated virus-mediated delivery of microRNA-21-3p lowers hypertension. *Mol Ther Nucleic Acids*. 2018;11:354–366.
8. Flamand MN, Wu E, Vashisht A, Jannot G, Keiper BD, Simard MJ, Wohlschlegel J, Duchaine TF. Poly(A)-binding proteins are required for microRNA-mediated silencing and to promote target deadenylation in *C. elegans*. *Nucleic Acids Res*. 2016;44:5924–5935.
9. Bartel DP. MicroRNAs: target recognition and regulatory functions. *Cell*. 2009;136:215–233.
10. Zhang X, Dong S, Jia Q, Zhang A, Li Y, Zhu Y, Lv S, Zhang J. The microRNA in ventricular remodeling: the miR-30 family. *Biosci Rep*. 2019;39.

11. Lapikova-Bryhinska T, Zhukovska A, Nagibin V, Tumanovska L, Portnichenko G, Goncharov S, Portnychenko A, Dosenko V. Altered biogenesis of microRNA-1 is associated with cardiac dysfunction in aging of spontaneously hypertensive rats. *Mol Cell Biochem*. 2019;459:73–82.

12. Yang X, Dong M, Wen H, Liu X, Zhang M, Ma L, Zhang C, Luan X, Lu H, Zhang Y. MiR-26a contributes to the PDGF-BB-induced phenotypic switch of vascular smooth muscle cells by suppressing Smad1. *Oncotarget*. 2017;8:75844–75853.

13. Wu W, Shang YQ, Dai SL, Yi F, Wang XC. MiR-26a regulates vascular smooth muscle cell calcification in vitro through targeting CTGF. *Bratisl Lek Listy*. 2017;118:499–503.

14. Chen L, Zeng W, Yang B, Cui X, Feng C, Wang L, Wang H, Zhou X, Li P, Lv F, et al. Expression of antisense of microRNA-26a-5p in mesenchymal stem cells increases their therapeutic effects against cirrhosis. *Am J Transl Res*. 2017;9:1500–1508.

15. Chen X, Xiao W, Chen W, Liu X, Wu M, Bo Q, Luo Y, Ye S, Cao Y, Liu Y. MicroRNA-26a and -26b inhibit lens fibrosis and cataract by negatively regulating Jagged-1/Notch signaling pathway. *Cell Death Differ*. 2017;24:1990.

16. Liang H, Xu C, Pan Z, Zhang Y, Xu Z, Chen Y, Li T, Li X, Liu Y, Huangfu L, et al. The antifibrotic effects and mechanisms of microRNA-26a action in idiopathic pulmonary fibrosis. *Mol Ther*. 2014;22:1122–1133.

17. Cuspidi C, Ciulla M, Zanchetti A. Hypertensive myocardial fibrosis. *Nephrol Dial Transplant*. 2006;21:20–23.

18. Guo Y, Gupte M, Umbarkar P, Singh AP, Sui JY, Force T, Lal H. Entanglement of GSK-3beta, beta-catenin and TGF-beta1 signaling network to regulate myocardial fibrosis. *J Mol Cell Cardiol*. 2017;110:109–120.

19. Wang LP, Fan SJ, Li SM, Wang XJ, Gao JL, Yang XH. Oxidative stress promotes myocardial fibrosis by upregulating KCa3.1 channel expression in AGT-REN double transgenic hypertensive mice. *Pflugers Arch*. 2017;469:1061–1071.

20. van Rooij E, Olson EN. MicroRNA therapeutics for cardiovascular disease: opportunities and obstacles. *Nat Rev Drug Discov*. 2012;11:860–872.

21. Melman YF, Shah R, Danielson K, Xiao J, Simonson B, Barth A, Chakir K, Lewis GD, Lavender Z, Truong QA, et al. Circulating microRNA-30d is associated with response to cardiac resynchronization therapy in heart failure and regulates cardiomyocyte apoptosis: a translational pilot study. *Circulation*. 2015;131:2202–2216.

22. Hinkel R, Penzkofer D, Zuhlke S, Fischer A, Husada W, Xu QF, Baloch E, van Rooij E, Zeiher AM, Kupatt C, et al. Inhibition of microRNA-92a protects against ischemia/reperfusion injury in a large-animal model. *Circulation*. 2013;128:1066–1075.

23. Wang B, Zhang A, Wang H, Klein JD, Tan L, Wang ZM, Du J, Naqvi N, Liu BC, Wang XH. miR-26a limits muscle wasting and cardiac fibrosis through exosome-mediated microRNA transfer in chronic kidney disease. *Theranostics*. 2019;9:1864–1877.

24. Gupta P, Sata TN, Ahamad N, Islam R, Yadav AK, Mishra A, Nithyananthan S, Thirunavukkarasu C, Sanal MG, Venugopal SK. Augmenter of liver regeneration enhances cell proliferation through the microRNA-26a/Akt/cyclin D1 pathway in hepatic cells. *Hepatol Res*. 2019;49:1341–1352.

25. Zhang S, Cui R. The targeted regulation of miR-26a on PTEN-PI3K/AKT signaling pathway in myocardial fibrosis after myocardial infarction. *Eur Rev Med Pharmacol Sci*. 2018;22:523–531.

26. Zheng L, Lin S, Lv C. MiR-26a-5p regulates cardiac fibroblasts collagen expression by targeting ULK1. *Sci Rep*. 2018;8:2104.

27. Zhao XY, Li L, Zhang JY, Liu GQ, Chen YL, Yang PL, Liu RY. Atorvastatin prevents left ventricular remodeling in spontaneously hypertensive rats. *Int Heart J*. 2010;51:426–431.

28. Sakai N, Nakamura M, Lipson KE, Miyake T, Kamikawa Y, Sagara A, Shinozaki Y, Kitajima S, Toyama T, Hara A, et al. Inhibition of CTGF ameliorates peritoneal fibrosis through suppression of fibroblast and myofibroblast accumulation and angiogenesis. *Sci Rep*. 2017;7:5392.

29. An E, Park H, Lee AC. Inhibition of fibrotic contraction by C-phycocyanin through modulation of connective tissue growth factor and alpha-smooth muscle actin expression. *Tissue Eng Regen Med*. 2016;13:388–395.

30. Xue M, Gong S, Dai J, Chen G, Hu J. The treatment of fibrosis of joint synovium and frozen shoulder by Smad4 gene silencing in rats. *PLoS One*. 2016;11:e0158093.

31. Pastuszak-Lewandoska D, Kordiak J, Czarnecka KH, Migdalska-Sek M, Nawrot E, Domanska-Senderowska D, Kiszalkiewicz JM, Antczak A, Gorski P, Brzezianska-Lasota E. Expression analysis of three miR-NAs, miR-26a, miR-29b and miR-519d, in relation to MMP-2 expression level in non-small cell lung cancer patients: a pilot study. *Med Oncol*. 2016;33:96.

32. He A, Ma Q, Cao J, von Gise A, Zhou P, Xie H, Zhang B, Hsing M, Christodoulou DC, Cahan P, et al. Polycomb repressive complex 2 regulates normal development of the mouse heart. *Circ Res*. 2012;110:406–415.

33. Mathiyalagan P, Okabe J, Chang L, Su Y, Du XJ, El-Osta A. The primary microRNA-208b interacts with Polycomb-group protein, Ezh2, to regulate gene expression in the heart. *Nucleic Acids Res*. 2014;42:790–803.

34. Hirai H, Kikyo N. Inhibitors of suppressive histone modification promote direct reprogramming of fibroblasts to cardiomyocyte-like cells. *Cardiovasc Res*. 2014;102:188–190.

35. Lu J, He ML, Wang L, Chen Y, Liu X, Dong Q, Chen YC, Peng Y, Yao KT, Kung HF, et al. MiR-26a inhibits cell growth and tumorigenesis of nasopharyngeal carcinoma through repression of EZH2. *Cancer Res*. 2011;71:225–233.

36. Seward S, Semaan A, Qazi AM, Gruzdyn OV, Chamala S, Bryant CC, Kumar S, Cameron D, Sethi S, Ali-Fehmi R, et al. EZH2 blockade by RNA interference inhibits growth of ovarian cancer by facilitating re-expression of p21(waf1/cip1) and by inhibiting mutant p53. *Cancer Lett*. 2013;336:53–60.

SUPPLEMENTAL MATERIAL

Table S1. Gene-specific primer sequences.

	Gene-specific primer sequence
miR-26a of rats-Forward	5'-TTCAAGTAATCCAGGATAGGCT-3'
miR-26a of rats-Reverse	5'-CCTATTCTTGGTTACTTGCAC-3'
miR-26a of mice-Forward	5'-GGGCTCTTTCCTTAGACTTGG-3'
miR-26a of mice-Reverse	5'-GACCTGCTTTGCTCATAACACTC-3'
U6-Forward	5'-GGAACGATACAGAGAAGATTAGC-3'
U6-Reverse	5'-TGGAACGCTTCACGAATTTGCG-3'
Col I-Forward	5'-TCCTGCCGATGTCGCTATCC-3'
Col I-Reverse	5'-TCGTGCAGCCATCCACAAGC-3'
Col III-Forward	5'-GCCTTCTACACCTGCTCCTG-3'
Col III-Reverse	5'-AGCCACCCATTCCTCCGACT-3'
MMP2-Forward	5'-CCAAGAACTTCCGACTATCC-3'
MMP2-Reverse	5'-GTCACTGTCCGCCAAATAAA-3'
TGFβRI-Forward	5'-TCGCCCTTTCATTTCAGA-3'
TGFβRI-Reverse	5'-TTTGCCGATGCTTTCTTG-3'
CTGF-Forward	5'-TGCTGTGAGGAGTGGGTGT-3'
CTGF-Reverse	5'-GCTCGCATCATAGTTGGGT-3'
Smad4-Forward	5'-CACTATGAGCGGGTTGTC-3'
Smad4-Reverse	5'-GTGGGTAAGGATGGCTGT-3'
EZH2-Forward	5'-GGACACTCCTCCAAGAAA-3'
EZH2-Reverse	5'-GGTCACAGGGTTGATAGTT-3'
β-actin-Forward	5'-GGAGATTACTGCCCTGGCTCCTAGC-3'
β-actin-Reverse	5'-GGCCGGACTCATCGTACTCCTGCTT-3'

Table S2. Conditions for amplification of qPCR.

miR-26a			mRNA		
95°C	10 s	for 1 cycle	95°C	2 min	for 1 cycle
95°C	5 s		95°C	10 s	
		for 40 cycles	60°C	20 s	for 33 cycles
60°C	20 s		72°C	30 s	
95°C	1 min				
55°C	30 s	for 1 cycles			
95°C	30 s				